

# BROS

## *A New Robotic Platform for the Treatment of Supracondylar Humerus Fracture*

Ben Salem Mohamed Oussama<sup>1,2</sup>, Mosbahi Olfa<sup>1,4</sup>, Khalgui Mohamed<sup>1,4</sup> and Frey Georg<sup>3</sup>

<sup>1</sup>LISI laboratory, INSAT, University of Carthage, Tunis, Tunisia

<sup>2</sup>Polytechnic School of Tunisia, University of Carthage, Tunis, Tunisia

<sup>3</sup>Saarland University, Chair of Automation, Saarbrücken, Germany

<sup>4</sup>eHealth Technologies Consortium, eHTC, Tunisia

**Keywords:** Supracondylar Humerus Fracture, Robot-assisted Surgery, E-Health, Reconfiguration.

**Abstract:** The supracondylar humerus fracture is one of the most common and challenging injury faced by pediatric orthopedic surgeons. Its treatment may lead to many neurological and vascular complications. This is mainly due to the "blind" pinning performed by surgeons to fix the fractured elbow's fragments. Furthermore, the medical staff is usually exposed to a high level of radiations during the surgery because of the fluoroscopically assisted treatment. Thus, a new robotized platform baptized BROS is developed in Tunisia to remedy this issue and allow performing a safer surgery. BROS is reconfigurable and may run under several operating modes, meeting, thus, the surgeon's requirements and the environment constraints. This paper introduces this new robotic platform and a real case of robot-assisted surgery is simulated to check the performances of BROS.

## 1 INTRODUCTION

The field of robotics is expanding day after day. The ability of robots to replace, supplement or transcend human performance has had a profound influence on many fields of our society, spanning fields such as agriculture, military and especially medicine. Patients demand greater precision, less and minimally invasive procedures, and faster recovery times. The increasing life expectancy associated with a need for reducing costs and increasing efficiency have opened the door for new and innovative solutions in the medical robotic industry. The field of computer-assisted surgery is relatively new since the first clinical application of a robot was performed to a neurosurgery in 1985 (Kwoh et al., 1988). Since then, many research centers around the world have developed a multitude of robotic surgical products to tackle new areas such as ophthalmology, radiology, urology, cardiothoracic and orthopedics (Cleary and Nguyen, 2001).

One of the most common injuries faced by pediatric orthopedic surgery is the supracondylar fracture of the humerus (or SCH). It accounts for 18% of all pediatric fractures and 75% of all elbow fractures (Landin and Danielsson, 1986). It mainly

occurs during the first decade of life and are more common among boys (Landin, 1983). The current treatment of SCH may lead to many complications. The neurological ones consists in damages caused to the median nerve during the reduction of the fracture or during the open procedure. The study in (Gosens and Bongers, 2003) also reports some vascular complications, mostly consisting in the disruption of the brachial artery. All those complications are principally caused by the "blind" pinning the surgeons perform (Flynn et al., 1974). Even though they are usually using an image intensifier, the medical staff can't guess in advance the trajectory the pin will follow. Images are actually taken once the pin is inserted, which may cause the previously mentioned complications. Other inconvenient of the current treatment technique is the recurrent medical staff exposure to radiations when using the fluoroscopic C-arm (Clein, 1954). These X-ray Radiations are harmful, and fluoroscopic examinations usually involve higher radiation doses than simple radiography. For example, a work in (Rampersaud et al., 2000) showed that, for spine surgeons, radiation exposures may approach or exceed guidelines for cumulative exposure. Another research in (Haque et al., 2006) showed that the

fluoroscopically assisted placement of pedicle screws in adolescent idiopathic scoliosis may expose the spine surgeon to radiation levels that exceed established lifetime dose equivalent limits.

Considering these constraints and issues, a new national project, baptized BROS (Browser-based Reconfigurable Orthopedic Surgery), has been launched to remedy these problems. BROS a new reconfigurable robotized platform dedicated to the treatment of supracondylar humeral fractures. It is capable of running under several operating modes to meet the surgeon's requirements and well-defined constraints. Thus, it can whether automatically perform the whole surgery or bequeath some tasks to the surgeon. BROS architecture is composed of a control unit, a browsing system with a middleware to perform image processing, two robotic arms to reduce the fracture and another one to insert pins in the fractured elbow.

This paper is organized as follows: the next section describes useful preliminaries for the reader. Section 3 introduces a real case study of a surgery undergone by a patient suffering from SCH to show the limit of the current fracture treatment. We expose, in Section 4, our robotic platform and its functioning. Section 5 presents the developed middleware, while Section 6 introduces the control unit of BROS. We finish the paper in Section 7 by a conclusion and an exposition of our future works.

## 2 BACKGROUND

We start, in this section, by presenting the robotic arm that we will use to implement BROS and the used software to configure it. We expose, thereafter, an overview about the different classifications of the supracondylar humerus fracture.

### 2.1 Platform and Environment

As the smallest robot from ABB, the IRB 120 offers all the functionality and expertise of the ABB range in a much smaller package. Like all ABB robots, the IRB 120 is a particularly agile 6-axis robot which, thanks to its compact turning radius, can be mounted closer to other equipment. Besides, it is ideal for a wide range of industries including the electronic, food and beverage, machinery, solar, pharmaceutical, medical and research sectors. With its lightweight but strong aluminum structure and small powerful engines, the IRB 120 weighs only 25 kg, which explains its rapid and precise acceleration. In fact, this featherweight has all the traditional

features of ABB robots, including leading performance in terms of trajectory tracking and motion control. Thus, the IRB 120 won many manufacturers' spurs (Emmerson, 2011; Cardwell, 2011).

IRB 120 can be programmed offline with RobotStudio ABB's software that allows to simulate an industrial manufacturing cell to find the optimal position of the robot and avoid costly downtime and production delays (Mikaelsson and Curtis, 2009). RobotStudio from ABB Robotics is a powerful off-line robot programming and simulation tool. What makes it unique is the fact that, when the code is fully developed off-line, it downloads to the actual controller with no translation stage, reducing time-to-market. RobotStudio is able to create the robot movements using graphical programming, edit and debug the robot system, and simulate and optimize existing robot programs. It is widely used in universities to educate engineering students in the capabilities and applications of robots, as well as in the automation industry by mechanical designers and robot programmers. RobotStudio is also used in remote maintenance and troubleshooting. It actually connects to the live system to take an instant virtual copy, and then goes off-line to enable the situation to be studied in depth. RobotStudio also features a RAPID Editor which enables the user to write a robot program. The user can watch a single robot execute the RAPID program in the graphical environment (Connolly, 2009).

### 2.2 Classification of Supracondylar Humeral Fracture

Many classifications of the supracondylar humeral fractures were established. They are based on both the direction and the degree of displacement of the distal fragment (Barton et al., 2001). The Lagrange classification system and the Gartland's are the most widely used. The first is the most widely used in the French literature. It divides these fractures into four types on the basis of antero-posterior and lateral radiographs (Lagrange and Rigault, 1962). In the English literature, the second is the most commonly used: the Gartland's classification is based on the lateral radiograph and fractures are classified, as illustrated in Figure 1, according to a simple three-type system (Table 1) (Pirone et al., 1988). We adopt this classification in this paper.

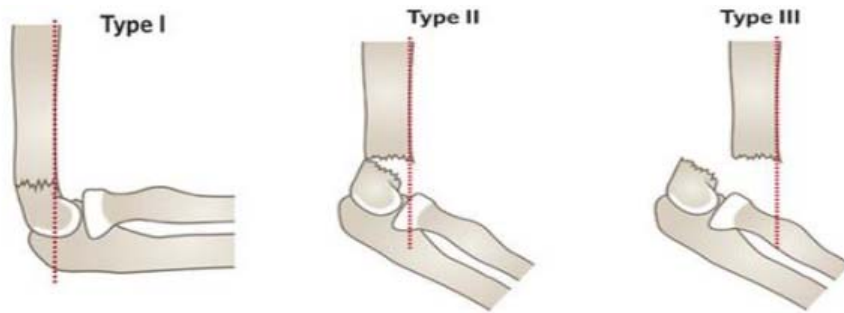


Figure 1: Gartland's classification of supracondylar fractures of the humerus.

Table 1: Gartland's classification of supracondylar fractures of the humerus.

Type	Radiologic characteristics
I	Undisplaced fractures
II	Displaced fracture with intact posterior hinge
III	Completely displaced fractures with no contact between the fragments

anesthesia and fluoroscopic control. First, a radiography of the injured elbow is taken to determine the type of fracture. The latter was found a type III fracture according to Gartland's classification as show in Figure 2.

The patient, anesthetized, is then placed under the fluoroscopic image intensifier (Figure 3).

### 3 CASE STUDY

We expose, in this section, a true case of a patient suffering from a supracondylar humeral fracture who came to the Children Hospital of Béchir Hamza (Tunis). The patient who is a ten-year-old girl fell on her outstretched right hand on November 12<sup>th</sup> 2013. Once supported, the patient's elbow was placed in a brace in a 20-to-40° flexion to promote vascularization of the organ. She underwent a surgery on the same day. We were invited by Prof.Dr.med. Mahmoud Smida, the head of Child and Adolescent Orthopedics Service and our medical collaborator, to attend the intervention.

Treatment with single traction is not considered any more in modern centers due to a long required hospitalization and excellent current surgical results. The closed reduction with pinning is now the most used technique. It is performed under general



Figure 3: The patient installed under the fluoroscopic image intensifier.

The fracture is reduced in the frontal plane in extension and the elbow is bent while pushing forward the olecranon. The surgeon repeatedly rotated the image intensifier rather than the limb and took a total of 9 images to verify the reduction profile. The limb is immobilized once a satisfying reduction is obtained (Figure 4).



Figure 2: The fracture's radiography.



Figure 4: Limb immobilization.

Two percutaneous pinning are finally performed in the distal fragment as illustrated in Figure 5 to fix the bone and avoid any risk of cubitus varus (a common deformity in which the extended forearm is deviated towards midline of the body). To avoid any vascular or nerve injury during the insertion of the two pins, 15 fluoroscopic images were taken.



Figure 5: Percutaneous pinning.

During this surgery, a total of 24 fluoroscopic images was taken, which involves high doses of radiation to the medical staff, especially since such interventions are performed 5 times per day on average. The second pin had to be removed and reinserted since it didn't straightaway follow the right trajectory, which can lead to some complications. To remedy these problems, we launch a new project, baptized BROS, which

consists in a robotized platform to automatically perform such surgeries or assist the surgeon by limiting his exposition to radiations and bypassing the blind pinning issue.

## 4 BROS

BROS is a new and original robotic platform. This project was launched to remedy the two most important difficulties the medical staff is facing: the blind pinning and the recurrent exposure to radiations.

We present in this section the BROS's architecture and its operating modes.

### 4.1 Architecture

BROS is a robotic platform dedicated to humeral supracondylar fracture treatment. It is able to reduce fractures, block the arm and fix the elbow bone's fragments by pinning. It also offers a navigation function to follow the pins' progression into the fractured elbow.

BROS is, as shown in the class diagram hereafter, composed of a browser (BW), a control unit (UC), a middleware (MW), a pinning robotic arm (P-BROS) and 2 blocking and reducing arms (B-BROS1 and B-BROS2). The said components are detailed hereafter.

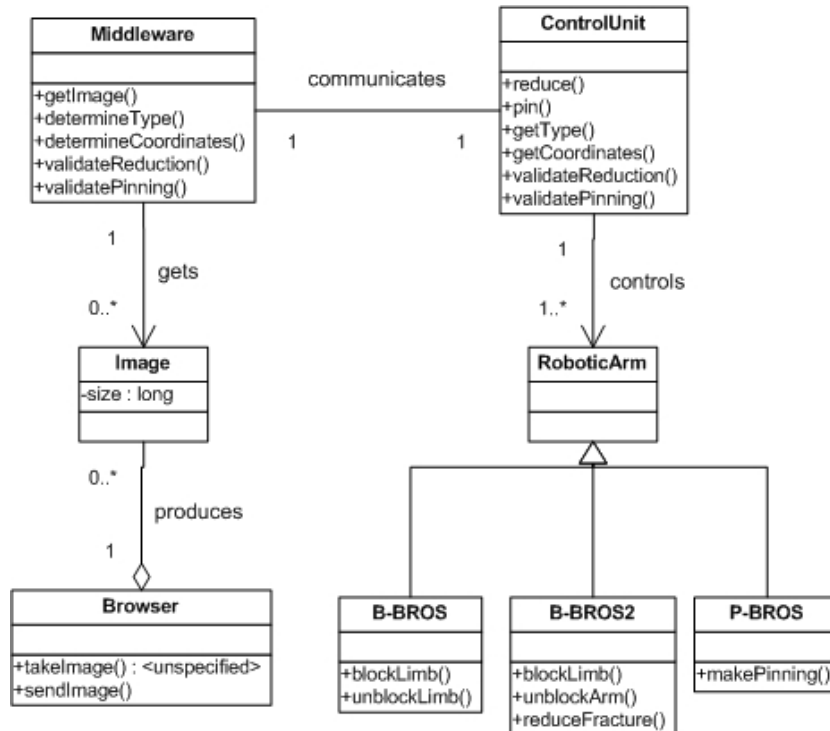


Figure 6: BROS's class diagram.

### Browser

The browser, which is a Medtronic's product and called FluoroNav, is a combination of specialized surgical hardware and image guidance software designed for use with a StealthStation Treatment Guidance System. Together, these products enable a surgeon to track the position of a surgical instrument in the operating room and continuously update this position within one or more still-frame fluoroscopic images acquired from a C-Arm. The advantages of this "virtual" navigation over conventional fluoroscopic navigation include: (i) the ability to navigate using multiple fluoroscopic views simultaneously, (ii) the ability to remove the C-Arm from the operative field during navigation, (iii) significant reduction in radiation exposure to the patient and staff.

In addition, the FluoroNav System allows the surgeon to: (i) simulate and measure instrument progression or regression along a surgical trajectory, (ii) save instrument trajectories, and display the angle between two saved trajectories or between a saved trajectory and the current instrument trajectory, (iii) measure the distance between any two points in the camera's field of view, (iv) measure the angle and distance between a surgical instrument and a plane passing through the surgical field (such as the patient midplane).

Primary hardware components in the FluoroNav System include the FluoroNav Software, a C-Arm Calibration Target, a reference frame, connection cables, and specialized surgical instruments.

### Control Unit

The CU ensures the smooth running of the surgery and its functional safety. It asks the supracondylar fracture's type to the middleware, and then computes, according to it, the different coordinates necessary to specify the robotic arms' behaviors concerning the fracture's reduction, blocking the arm and performing pinning. The surgeon monitors the intervention progress thanks to a dashboard installed on the CU.

### Middleware

The middleware is a software installed on the browser and which acts as a mediator between the CU and the BW. It is an intelligent component that provides several features of real-time monitoring and decision making. The middleware contains several modules which are fully explained in Section 5: (i) an image processing module, (ii) a controller, (iii) a communication module with the CU.

### Pining Robotic Arm

The pinning robotic arm, P-BROS, inserts two parallel Kirschner wires according to Judet technique (Judet, 1953) to fix the fractured elbow's fragments. To insure an optimal postoperative stability, BROS respects the formula:

$$S = \frac{B}{D} > 0.22 \quad (1)$$

where  $S$  is the stability threshold,  $B$  the distance separating the two wires and  $D$  the humeral palette's width (Smida et al., 2007).

### Blocking and Reducing Robotic Arms

B-BROS1 blocks the arm at the humerus to prepare it to the fracture reduction. B-BROS2 performs then a closed reduction to the fractured elbow before blocking it once the reduction is properly completed.

## 4.2 Reconfiguration and Operating Modes

Reconfiguration is an important feature of BROS. It is designed to be able to operate in different modes. The surgeon can actually decide to manually do a task if BROS does not succeed to automatically perform it, whether it is fracture reduction, blocking the arm or pinning the elbow. Thus, five different operating modes are designed and detailed hereafter: (i) Automatic Mode (AM): The whole surgery is performed by BROS. The surgeon oversees the operation running, (ii) Semi-Automatic Mode (SAM): The surgeon reduces the fracture. BROS performs the remaining tasks, (iii) Degraded Mode for Pining (DMP): BROS only realizes the pinning. It's to the surgeon to insure the rest of the intervention, (iv) Degraded Mode for Blocking (DMB): BROS only blocks the fractured limb. The remaining tasks are manually done by the surgeon, (v) Basic Mode (BM): The whole intervention is manually performed. BROS provides navigation function using the middleware that checks in real time the smooth running of the operation.

## 4.3 Humeral Supracondylar Fracture Treatment

To treat a humeral supracondylar fracture using BROS, the following steps are performed in the automatic mode:

- i. the surgeon launches the system and chooses one of the five operating modes;
- ii. CU asks MW about the fracture coordinates;
- iii. MW requests an image from BW and the latter sends it;

- iv. MW determines the different coordinates by image processing and sends them to CU;
- v. based on the received coordinates, CU orders B-BROS1 to block the arm at the humerus;
- vi. B-BROS1 blocks the limb;
- vii. CU asks B-BROS2 to reduce the fracture based on the latter's line;
- viii. B-BROS2 reduces the fracture;
- ix. CU asks MW to ensure that the reduction was successful;
- x. MW requests a new image from BW and checks the fracture reduction result. If it is satisfactory, BROS moves to step xi. Steps from vii. to ix. are repeated otherwise;
- xi. CU orders B-BROS2 to block the arm;
- xii. under the request of UC, P-BROS performs the first and the second pinning;
- xiii. once the pinning is successful, CU asks B-BROS1 and B-BROS2 to unblock the limb.

**Running example 1**

To test our new robotized platform, we decided to simulate the surgery that would be performed on a real case. Thus, we chose a new patient, a nine-year-old girl, suffering from a fracture similar to the one presented in the case study of Section 3 (a type III fracture). We simulated the whole surgery on June 9<sup>th</sup> 2014 using the software RobotStudio and the developed middleware and control unit. We will present the obtained results as we introduce these two components in the next sections.

**5 MIDDLEWARE**

We introduce in this section the architecture of the middleware and its image processing module.

**5.1 Architecture**

The Middleware features two important modules: the first performs operations relating to image processing and the second insures the synchronization and communication with the whole robotized platform. Middleware's class diagram is illustrated in Figure 7.

Since the middleware acts as a mediator between the browser and the control unit, several data are exchanged between MW and CU during the surgery. First, the control unit notifies the start of the intervention and the activated operating mode to the middleware. Then, it asks it to compute necessary parameters like fracture's type and spatial coordinates. It also informs MW about the end of

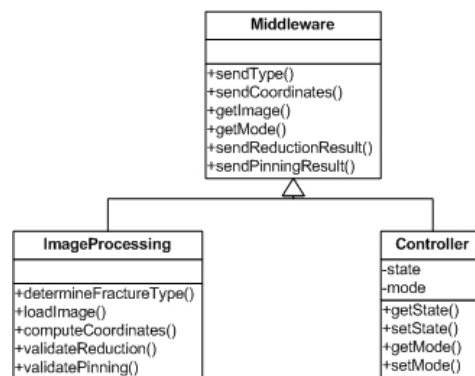


Figure 7: Middleware's class diagram.

reduction and pinning. The middleware and the control unit are connected through an ad hoc network. We illustrate the different exchanges between MW and CU by a sequence diagram as shown in Figure 8.

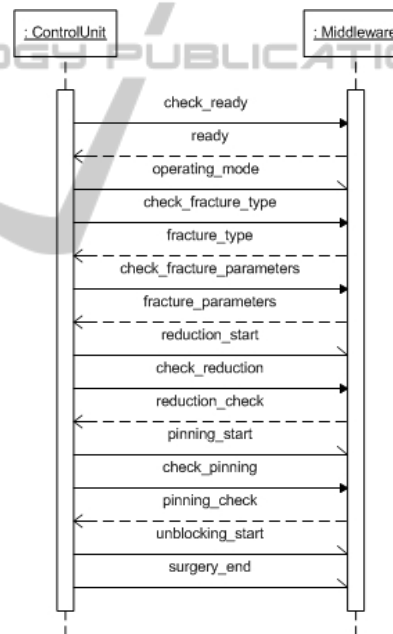


Figure 8: Sequence diagram of communication with CU.

The controller is a module that saves the current status reached by the intervention. Indeed, the control unit informs the middleware of each fired transition and the current triggered operating mode. The control unit updates these information as the intervention advances in time. Thus, the middleware is kept aware of the progress of the surgery. This module synchronizes, then, the middleware with the whole operation.

The image processing module is deeply detailed in the next section.

## 5.2 Image Processing

Image processing is the most important module of the middleware and provides a number of features that we detail below.

### Locating

Locating is an important feature that involves setting a spatial reference which is considered during the whole intervention. The middleware and the control unit must use the same coordinate system since several points' coordinates computed by MW are, firstly, sent to CU so the latter performs a preoperative simulation and, secondly, to B-BROS and P-BROS to realize the fracture reduction and pinning. We choose to fix the coordinate system origin at the patient's elbow as illustrated in Figure 9. The X, Y and Z axes respectively represent the elbow's rotation axis, the humeral palette length's median and the normal to (XY) plan.

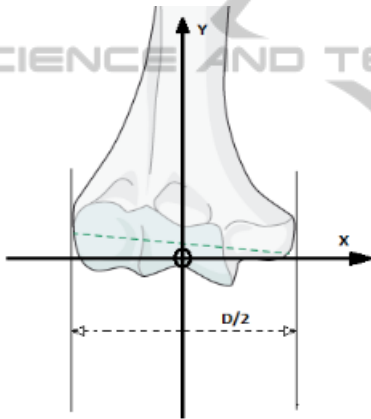


Figure 9: The coordinate system axes.

### Determination of the Fracture Type

MW starts by receiving from BW a first image of the fracture to determine its type. It compares the acquired image with the ones stored in its database. To do this, the middleware uses two image processing techniques, ensuring, thus, proper detection of the fracture type. The first one is image matching and consists in comparing images in order to obtain a measure of their similarity. It extracts invariant local features for all images, and then uses voting to rank the database images in similarity with the query image (Grauman and Darrell, 2005). The second used image processing technique is contour comparison. It consists in detecting an image contour by quantifying the presence of a boundary at a given image location through local measurements (Arbelaez et al., 2011). The contour comparison is

applied on the patient's elbow image acquired from BW and images stored at the database, one at a time.

### Running example 2

Figure 10 shows the result of image matching applied on the running example's fractured elbow (on the left) and an image from the MW database (on the right). Figure 11, for its part, shows a contour comparison with another image from the database. The type III is confirmed.

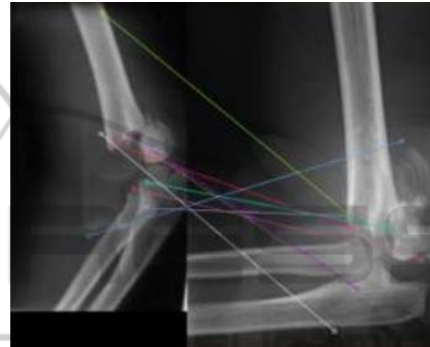


Figure 10: Image matching applied on two fractured elbow images.

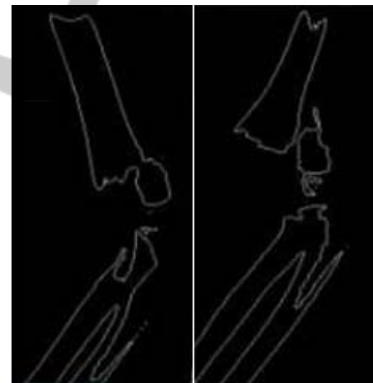


Figure 11: Contour comparison performed by MW.

### Coordinates Transformation

The middleware acquires images from the browser. The latter uses a system camera composed of two lenses to geometrically triangulate the spatial coordinates of each light source on the instrument, reference frame, and C-Arm Target. However, the images it sends to MW are two-dimensional, and MW needs to operate in a three-dimensional environment to properly ensure the different steps of the surgery, such as the fracture reduction and pinning. Thus, we must, first, realize a camera calibration which consists in finding the relationship between the spatial coordinates of a point in space

(i.e. the operating theatre) and the associated point in the image taken by the camera (Tsai, 1987). To achieve the desired transformation, two type of parameters must be determined:

- the camera extrinsic parameters which define the position and orientation of camera relative to the space in which we work. Technically, determining these parameters consists in finding the translation vector between the relative positions of the origins of two references: the camera reference and the operating theatre's. A rotation vector aligning the axes of the two references must also be computed.
- the camera intrinsic parameters which are required to bind the image pixels coordinates with the corresponding ones in the camera coordinate system. These parameters present the camera optical, digital and geometric features like the focal length, the geometric distortion and image magnification factors.

Figure 12 illustrates the different used coordinate systems where: (i)  $(x, y)$  plan is the image pixels reference, (ii)  $(x', y', z')$  is the camera coordinate system, (iii)  $(x, y, z)$  is the operating theatre reference.

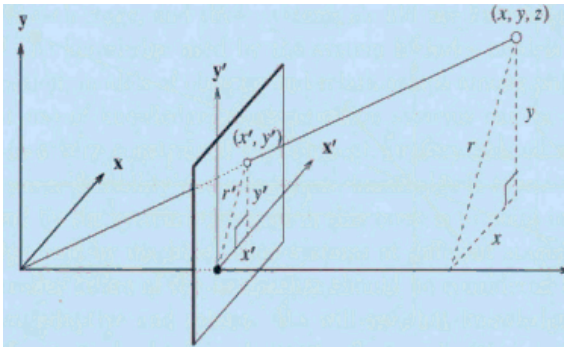


Figure 12: The different coordinate systems.

To translate the coordinates of a point in the image from the latter's reference to the operating theatre's and vice versa, we use the following formula:

$$S \begin{bmatrix} u \\ v \\ 1 \end{bmatrix} = M \left( R \begin{bmatrix} X \\ Y \\ Z_{const} \end{bmatrix} + T \right) \quad (2)$$

where : (i)  $S \begin{bmatrix} u \\ v \\ 1 \end{bmatrix}$  are the coordinates of a point in the image, (ii)  $M$  is the camera matrix, (iii)  $R$  represents the rotation vector, (iv)  $T$  is the translation vector, (v)  $(X, Y, Z_{const})$  are the coordinates corresponding to the point  $S$  in the operating theatre reference.

### Fracture Reduction Validation

The validation of fracture reduction consists in checking whether the bone fragments regained their original places or not. Thus, this module detects, based on the acquired image, the bone discontinuity and, then, computes the distance between the displaced bone fragments. We hereafter explain this technique with the most common fracture types of Lagrange classification: II and III.

Validating the reduction of a type II fracture involves calculating the distances  $AC$  and  $BD$  as illustrated in Figure 13. A reduction is considered successful when:

$$|AC| = |BD| = 0 \quad (3)$$

BROS has only three attempts to achieve a successful reduction before switching to the semi-automatic mode (SAM) to let the surgeon manually perform it.

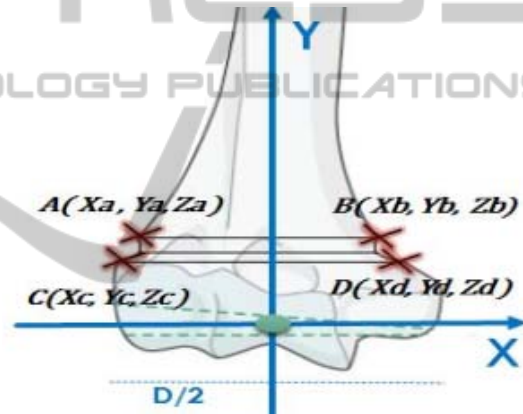


Figure 13: The reduction of a type II fracture.

The type III fractures usually present a rotary disorder. Their reduction consists, therefore, in the rotation of the forearm with an  $\alpha$  angle which is  $\arcsin(Z_b - Z_a)$  as illustrated in Figure 14.

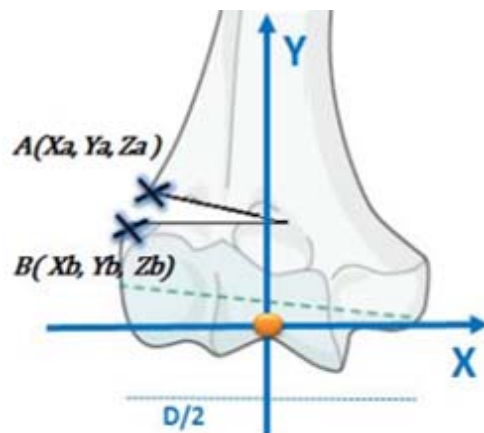


Figure 14: The reduction of a type III fracture.

**Pinning Validation**

Pinning validation amounts to checking the respect of the formula 1 introduced in section 4.1 by computing the humeral palette's width and the distance separating the two pins.

**6 CONTROL UNIT**

The control unit, the entity responsible of the smooth running and the safety of surgery, is composed of several modules which we detail hereafter. We use RobotStudio to implement it and RobotWare (Robotics, 2007) as the robot controller. Both are ABB's products.

**6.1 Station Definition**

This module implements the station which is, in our case, the operating room with all its components. The latter can be grouped into two categories: the mechanisms and the static components. The mechanisms are objects that perform 3D motion during simulations, whereas static components, as their name suggests, remain fixed during all surgery.

**Running example 3**

Figure 15 shows the implementation of our operating theater with its different robotic arms, the patient's limb modeling and the surgical bed.

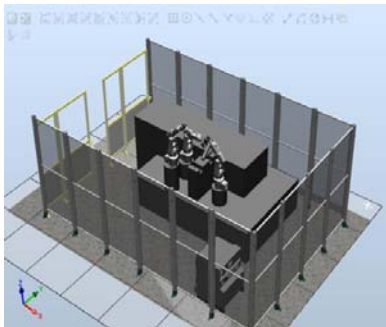


Figure 15: The operating room definition.

**Mechanisms**

Our operating theatre's mechanisms are B-BROS1, B-BROS2 and PBROS. They are all ABB's IRB 120 which we earlier presented in section 2.1. "Blocker 1" is the used tool to block the patient's limb at humerus and lately unblock it according to coordinates computed by the blocking module. To reduce the fracture and block the limb at forearm, "Blocker 2" is used according to coordinates

received from the reduction module. Blocker 1 and Blocker 2 have the same 3D modeling illustrated in Figure 16.

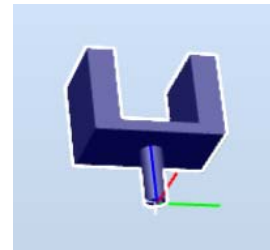


Figure 16: Blocker 1 and Blocker 2's 3D modeling.

"Pinning", as its name suggests, is the used tool to perform pinning at the patient's elbow according coordinates computed by the pinning module. Its 3D modeling is showed in Figure 17.



Figure 17: Pinning's 3D modeling.

To simulate the progress of the surgery on the patient's limb, we model the latter as illustrated in Figure 18. It is modeled by a mechanism that rotates about the X axis (in red).

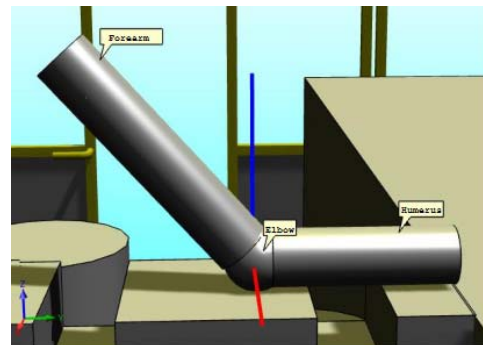


Figure 18: Limb's 3D modeling.

**Static Components**

Static components are the different 3D objects which are useful to the simulation like the robotic arms' racks and the surgical bed.

## 6.2 B-BROS1 Module

B-BROS1 module describes the behavior of the robotic arm B-BROS1 and how it blocks the patient's limb at the humerus and unblocks it once the surgery is completed. Thus, this module features two procedures: (i) `B_BROS1_humerusBlock ()` : it blocks the arm at a distance of  $y+100$  mm where  $y$  is the coordinate on Y axis of the intersection point of the humeral palette and its median. Figure 19 illustrates how the blocking is performed, (ii) `B_BROS1_humerusUnblock ()`: it releases the patient's limb once the fracture treatment is completed.

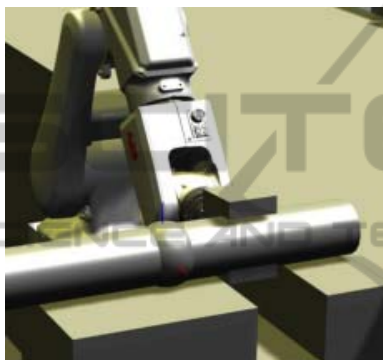


Figure 19: Blocking the patient's limb.

## 6.3 B-BROS2 Module

This module features several procedures which allow robotized fracture reduction when the automatic mode is triggered and direct robotized arm blocking when AM, SAM or DMB is triggered. B-BROS2 module releases the patient's limb once the surgery is completed. We, hereafter, detail the procedures: (i) `B_BROS2_reduce_II (A, B, C, D)` : it performs the reduction of a type II fracture and takes into account the parameters that we defined in Section 5.2. Figure 20 illustrates a robotized fracture reduction, (ii) `B_BROS2_unblock_II ()`: this procedure unblock the patient's limb suffering from



Figure 20: Robotized fracture reduction.

a type II fracture once the surgery is completed, (iii) `B_BROS2_reduce_III (A, B)`: it computes the rotation angle of the rotary disorder in the case of a type III fracture and, then, reduces the latter, (iv) `B_BROS2_block ()` : the procedure blocks the limb at the forearm once a manual reduction is performed during SAM or DMB. Figure 21 shows how this is performed.

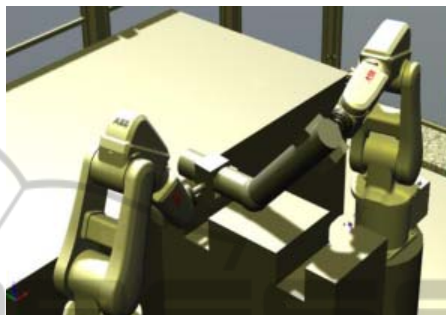


Figure 21: Blocking the fractured limb at the forearm.

## 6.4 P-BROS Module

This section describes the behavior of P-BROS, the robotic arm performing fracture reduction according to its type and the triggered operating mode. We point out that the used pinning technique is Judet's which we mentioned in Section 4.1. The orientation of the tool "Pinning" (Section 6.1), relatively to the coordinate system defined in Section 5.2, depends on the type of the fracture. Thus, the figures 22 and 23 respectively shows the orientation of "Pinning" in the case of a type II and a type III fractures.

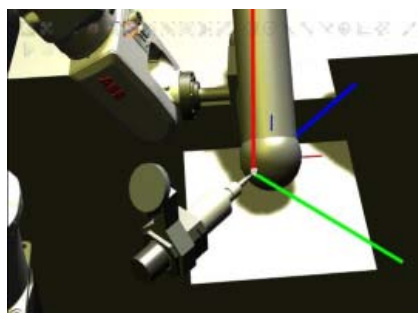


Figure 22: Orientation of "Pinning" in the case of a type II fracture.

The P-BROS module features several procedures that we hereafter detail: (i) `P_BROS_DoublePin (A, B, C, D, HP)` : it performs a parallel pinning using two pins inserted from the external condyle to the lateral humeral column in the case of a type II fracture which requires a double pinning. The procedure uses as parameters the four points of the

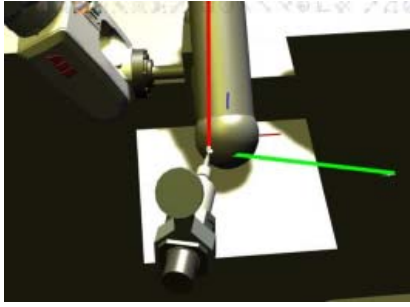


Figure 23: Orientation of "Pinning" in the case of a type III fracture.

distal dissolution and the width of the humeral palette (HP), (ii) P\_BROS\_SinglePin\_III (A, B, HP) : this procedure performs a percutaneous pinning for a type III fracture. The pin is actually inserted from the external condyle throughout the medial column in a rectilinear direction by keeping a fixed (XY) plane, (iii) P\_BROS\_SinglePin\_IV (A, B, HP) : it realizes a percutaneous pinning for a type IV fracture. Indeed, for this type of fracture, the pin is inserted in the lateral condyle and makes an angle of  $45^\circ$  relative to the orientation of the pin in the case of a type III fracture. The pin is inserted until reaching the lateral column.

## 6.5 Synchronization Module

We present, in this section, the synchronization module of the control unit. It is the entity that insures the coordination between the tasks of B-BROS1, B-BROS2 and P-BROS modules. To insure this function, we use interruptions through binary logic signals. Indeed, each signal corresponds to a very specific task. The signal is high when the task is running and low when it is idle or finished executing. We note that the used signals represent the steps of a fracture treatment based on the operating mode and regardless to the nature of a given action (robotized or manual).

We define for the control unit the following logic signals which we detail in Table 2:

Table 2: Synchronization logic signals.

Logic Signal	Description
HandBlocking	This signal controls the first step of a fracture treatment which is blocking the patient's limb at the humerus. It is the highest priority task. The signal is high when B-BROS1 starts blocking the humerus and it switches to low once blocking is finished.

Table 2: Synchronization logic signals (cont.).

HandReduction	The signal controls the fracture reduction and the forearm blocking. It switches to high when HandBlocking is low and either B-BROS2 starts the robotized reduction and/or blocking or the surgeon starts the manual reduction and/or blocking. It is the second priority task.
HandPinning	HandPinning controls pinning, whether it is manual or robotized. It changes to high when the signal HandReduction changes to low informing, thus, that reduction and blocking are finished. When it switches to high, HandPinning starts pinning and switches to low once it is finished.
HandUnblocking	It controls the limb unblocking, which is the lowest priority task.

## 6.6 CU-MW Communication Module

A good communication between the control unit and the middleware is critical to the smooth functioning of BROS. For example, the control unit cannot start the different processing until it receives key parameters like the fracture type and the coordinates of the points of the distal fragment discontinuity. The module respects the diagram presented in Section 5.1.

## 6.7 Surgeon-Robot Interface

It is the graphical interface through which the surgeon communicates with the platform and oversees the progress of the operation. The surgeon can, using this interface, choose the operating mode to start with. Through this GUI, the surgeon consults any medical parameter like the fracture type, the displacement nature or the angle of the rotational trouble in the case of type III fractures. This interface meets the man-machine requirements like: (i) Guidance: All resources used to guide the surgeon during the use of the interface like grouping/distinction, immediate feedback and legibility, (ii) Workload: Minimum and explicit actions ("start reduction", "start pinning"), informational density more or less acceptable for a surgeon, (iii) Error management: This is to protect sensitive actions against errors with error messages, (iv) Ergonomics: The interface must be flexible and adaptable to a surgeon and especially in an operating room.

**Running example 4**

The whole surgery was successfully performed by BROS under the automatic operating mode and simulated using RobotStudio and RobotWare. Only 4 fluoroscopic images were needed, what makes 21 images less than in the study case introduced in Section 3. BROS insured all the intervention steps and the surgeon had only to remotely check the smooth running of the surgery and be ready to intervene in the case where the robotized platform would not be able to perform one of the surgery's steps or he would judge that a human intervention is necessary.

## 7 CONCLUSION AND PERSPECTIVES

Our work consisted, through this paper, in introducing BROS, this new robotic platform dedicated to the treatment of supracondylar humerus fracture, and its contributions. BROS is a flexible system since it may run under different operating modes to meet the surgeon requirements and the environment constraints: it is reconfigurable. Through the simulation of a real case of BROS-assisted surgery, we proved the usefulness of this robotic platform to avoid the complications that may be generated because of the blind pinning and prevent the danger posed by the recurrent exposition to radiations. We can, now, certify that BROS is an innovating project which will be of a great help to pediatric orthopedic surgeons. The next step is to proceed to the real implementation of BROS using the ABB robotic arms.

## ACKNOWLEDGEMENTS

This research work is carried out within a MOBIDOC PhD thesis of the PASRI program, EU-funded and administered by ANPR (Tunisia). The BROS national project is a collaboration between the Children Hospital of Béchir Hamza (Tunis), eHTC and INSAT (LISI Laboratory) in Tunisia. We thank the medical staff, Prof.Dr.med. Mahmoud Smida (Head of Child and Adolescent Orthopedics Service) and Dr.med. Zied Jalia, for their fruitful collaboration and continuous medical support. A second paper is submitted in the conference for the modeling and verification of BROS.

## REFERENCES

- Arbelaez, P., Maire, M., Fowlkes, C., and Malik, J. (2011). Contour detection and hierarchical image segmentation. *Pattern Analysis and Machine Intelligence, IEEE Transactions on*, 33(5):898–916.
- Barton, K. L., Kaminsky, C. K., Green, D. W., Shean, C. J., Kautz, S. M., and Skaggs, D. L. (2001). Reliability of a modified Gartland classification of supracondylar humerus fractures. *Journal of Pediatric Orthopaedics*, 21(1):27–30.
- Cardwell, M. An irb 120 robots picks and packs tubes of hair color into boxes for l'oreal canada. [www.abb.com](http://www.abb.com).
- Cleary, K. and Nguyen, C. (2001). State of the art in surgical robotics: clinical applications and technology challenges. *Computer Aided Surgery*, 6(6):312–328.
- Clein, N. W. (1954). How safe is x-ray and fluoroscopy for the patient and the doctor? *The Journal of pediatrics*, 45(3):310–315.
- Mikaelsson, P. and Curtis, M. (2009). Portrait-robot d'un petit prodige: ABB présente son nouveau robot IRB 120 et son armoire de commande IRC5 Compact. *Revue ABB*, (4), 39–41.
- Connolly, C. (2009). Technology and applications of abb robotstudio. *Industrial Robot: An International Journal*, 36(6):540–545.
- Emmerson, B. Irb 120 inserting thermoplastic trays in to boxes for bdm. [www.abb.com](http://www.abb.com).
- Flynn, J. C., Matthews, J. G., Benoit, R. L., et al. (1974). Blind pinning of displaced supracondylar fractures of the humerus in children. *J Bone Joint Surg Am*, 56(2):263–72.
- Gosens, T. and Bongers, K. J. (2003). Neurovascular complications and functional outcome in displaced supracondylar fractures of the humerus in children. *Injury*, 34(4):267–273.
- Grauman, K. and Darrell, T. (2005). Efficient image matching with distributions of local invariant features. In *Computer Vision and Pattern Recognition, 2005. CVPR 2005. IEEE Computer Society Conference on*, volume 2, pages 627–634 vol. 2.
- Haque, M. U., Shufflebarger, H. L., O'Brien, M., and Macagno, A. (2006). Radiation exposure during pedicle screw placement in adolescent idiopathic scoliosis: is fluoroscopy safe? *Spine*, 31(21):2516–2520.
- Judet, J. (1953). Traitement des fractures sus-condyliennes transversales de l'humérus chez l'enfant. *Rev Chir Orthop*, 39:199–212.
- Kwoh, Y. S., Hou, J., Jonckheere, E. A., and Hayati, S. (1988). A robot with improved absolute positioning accuracy for ct guided stereotactic brain surgery. *Biomedical Engineering, IEEE Transactions on*, 35(2):153–160.
- Lagrange, J. and Rigault, P. (1962). Fractures supracondyliennes. *Rev Chir Orthop*, 48:337–414.
- Landin, L. A. (1983). Fracture patterns in children: Analysis of 8,682 fractures with special reference to incidence, etiology and secular changes in a swedish

- urban population 1950-1979. *Acta Orthopaedica*, 54(S202):3-109.
- Landin, L. A. and Danielsson, L. G. (1986). Elbow fractures in children: an epidemiological analysis of 589 cases. *Acta Orthopaedica*, 57(4):309-312.
- Pirone, A., Graham, H., Krajbich, J., et al. (1988). Management of displaced extension-type supracondylar fractures of the humerus in children. *J Bone Joint Surg Am*, 70(5):641-50.
- Rampersaud, Y. R., Foley, K. T., Shen, A. C., Williams, S., and Solomito, M. (2000). Radiation exposure to the spine surgeon during fluoroscopically assisted pedicle screw insertion. *Spine*, 25(20):2637-2645.
- Robotics, A. (2007). Application manual: Motion coordination and supervision, robot controller, robotware 5.0. Västerås, Sweden.
- Smida, M., Smaoui, H., Ben Jlila, T., Saeid, W., Safi, H., Ammar, C., Jalel, C., and Ben Ghachem, M. (2007). Un index de stabilité pour l'embrochage percutané latéral parallèle des fractures supracondyliennes du coude chez l'enfant. *Revue de Chirurgie Orthopédique et Réparatrice de l'Appareil Moteur*, 93(4):404.
- Tsai, R. Y. (1987). A versatile camera calibration technique for high-accuracy 3d machine vision metrology using off-the-shelf tv cameras and lenses. *Robotics and Automation, IEEE Journal of*, 3(4):323-344.

TECHNOLOGY PUBLICATIONS PRESS